Cyclic-AMP and Pseudosubstrate Effects on Type-I A-Kinase Regulatory and Catalytic Subunit Binding Kinetics†

Ganesh Anand,‡,|| Susan S. Taylor,‡ and David A. Johnson*,§

Departments of Chemistry/Biochemistry and Pharmacology and the Howard Hughes Medical Institute, University of California, San Diego, La Jolla, California 92037, and Division of Biomedical Sciences, University of California, Riverside, California 92521

Received March 1, 2007; Revised Manuscript Received June 8, 2007

ABSTRACT: To better understand the molecular mechanism of cAMP-induced and substrate-enhanced activation of type-I A-kinase, we measured the kinetics of A-kinase regulatory subunit interactions using a stopped-flow spectrofluorometric method. Specifically, we conjugated fluorescein maleimide (FM) to two separate single cysteine-substituted and truncated mutants of the type Iα regulatory subunit of A-kinase, RIα (91−244). One site of cysteine substitution and conjugation was at R92 and the other at R239. Although the emission from both conjugates changed with catalytic subunit binding, only the FM-R92C conjugate yielded unambiguous results in the presence of cAMP and was therefore used to assess whether a pseudosubstrate perturbed the rate of holoenzyme dissociation. We found that cAMP selectively accelerates the rate of dissociation of the RIα (91−244):C-subunit complex ∼700-fold, resulting in an equilibrium dissociation constant of 130 nM. Furthermore, excess amounts of the pseudosubstrate inhibitor, PKI(5−24), had no effect on the rate of RIα (91−244):C-subunit complex dissociation. The results indicate that the limited ability of cAMP to induce holoenzyme dissociation reflects a greatly reduced but still significant regulatory catalytic subunit affinity in the presence of cAMP. Moreover, the ability of the substrate to facilitate cAMP-induced dissociation results from the mass action effect of excess substrate and not from direct substrate binding to holoenzyme.

The regulatory (R^1) subunit of cAMP-dependent protein kinase (A-kinase) is a prototypic example of a signaling molecule that functions within the second messenger cyclic adenosine 3′5′-monophosphate (cAMP) pathway. The kinase core of A-kinase is the catalytic (C) subunit, which is a bilobal protein that is maintained in an inactive, tetrameric complex (R_2C_2, holoenzyme) with the dimeric R subunit. R subunits function both to confer cAMP dependence and to localize the holoenzyme to discrete subcellular locations via interactions with A-kinase anchoring proteins (AKAPs) (*1*).

There are two major R-subunit isoforms, RI and RII. Both isoforms are composed of four distinct functional domains: two cAMP binding domains (CNB-A and CNB-B), an inhibitory sequence that fits into the active-site cleft of the C subunit, and a dimerization/docking domain, which links R-subunit monomers and forms a docking surface for AKAPs (Figure 1A) (*2*). The inhibitory sequence for RII includes a substrate sequence that undergoes autophosphorylation in the presence of MgATP and cAMP, whereas RI has a pseudosubstrate sequence in which the P-site Ser is replaced with an Ala. R-subunit isoforms also differ in how they interact with the C subunit. For RI, only the inhibitory pseudosubstrate sequence and the CNB-A binding domain are essential for forming a high-affinity complex with the C subunit (*3*, *4*), and both the small and large lobes of the C subunit participate in the interaction. RII, however, interacts primarily with the larger C-subunit lobe, and both cAMP binding domains (CNB-A and CNB-B) are required for C subunit binding along with the inhibitory sequence (*5*). Additionally, R isoforms are associated with differential affinities toward AKAPs (*6*), hydrodynamic properties (*7*), and cAMP sensitivity to substrates (*8*). In the latter case, both peptidyl and macromolecular substrates shift the dose dependence of cAMP-induced activation to lower concentrations for RI but not for RII holoenzymes (*8*).

Clearly, enormous advances in A-kinase research have been made in the past three decades. Two current directions of research in this field involve understanding how the A-kinases fit into the plethora of signaling networks and elucidating the molecular mechanism of cAMP activation. We reasoned that both these research directions would benefit from a kinetic analysis of cAMP activation of A-kinases. As a first step toward this goal, we examined the kinetics of the C-subunit binding to RIα (91−244) in the absence and

† This work was supported by United States Public Health Service Grant GM19301 (to S.S.T.) and the Howard Hughes Medical Institute (S.S.T.).

* To whom correspondence should be addressed. Tel. (951) 827-3831. Fax: (951) 827-5504. E-mail: david.johnson@ucr.edu.

‡ University of California, San Diego.

§ University of California, Riverside.

|| Present address: Department of Biological Sciences, National University of Singapore.

[1] Abbreviations: C, catalytic subunit of protein kinase A; R, regulatory subunit of protein kinase A; A-kinase, cAMP-dependent protein kinase; RIα (91−244), deletion mutant of type Iα isoform of the R subunit; P, product; S, substrate; PKI(5−24), protein kinase A inhibitor fragment 5−24 amide trifluoroacetate salt; FM, fluorescein maleimide; SDS−PAGE, sodium dodecylsulfate−polyacrylamide gel electrophoresis; MES, (2-[*N*-morpholinoethanesulfonic acid) monohydrate; MOPS, 3-(*N*-morpholino)-propane-sulfonic acid.

10.1021/bi700421h CCC: $37.00
Published on Web 07/21/2007

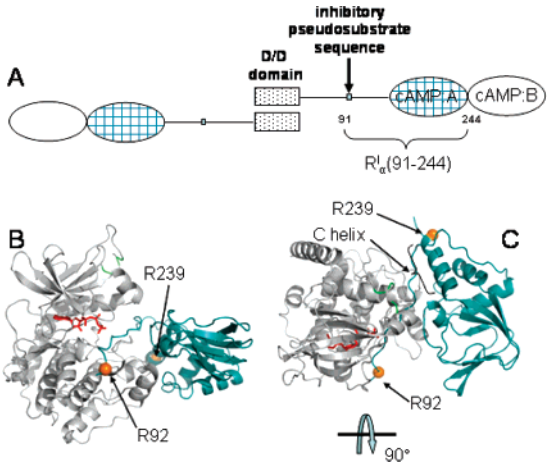

FIGURE 1: Structure of A-kinase RIα (91−244):C-subunit complex with sites of mutation and conjugation. (Panel A) Schematic delineating domain organization of A-kinase RIα. Each monomer of RIα is shown with an N-terminal dimerization/docking (D/D) domain, linker region containing an A-kinase pseudosubstrate inhibitory region (box), and two cAMP-binding domains (CNB-A, filled gradient ellipsoid and CNB-B, unfilled ellipsoid). (Panels B and C) Two perspectives (rotated 90° from each other) of the ribbon diagram of the structure of A-kinase RIα (91−244) in cyan complexed to the C subunit in gray with positions of the Arg-to-Cys mutations (R92C and R239C) highlighted (orange spheres) (*11*).

presence of cAMP and PKI(5−24) (a pseudosubstrate A-kinase inhibitor) by using stopped-flow fluorimetry combined with site-directed labeling. The doubly truncated RIα (91−244) was examined because residues 91−244 contain the pseudosubstrate sequence and CNB-A domain and alone account for all the binding energy associated with holoenzyme formation (K_d = 0.4 nM) (*9*, *10*). This makes RIα (91−244) an ideal system because the R−C interaction kinetics can be analyzed quantitatively, uncomplicated by the possible effects of the tethered target binding domains on the dimeric wild-type R subunit.

To develop a method to measure RIα (91−244)-C binding, two separate single cysteine-substituted RIα (91−244) mutants were engineered, labeled with fluorescein maleimide (FM), and evaluated for C-subunit binding-dependent changes in fluorescence. The sites of cysteine substitution were chosen on the basis of the X-ray crystal structure of the RIα (91−244):C complex (*11*) to be near but not part of the R−C binding interface. The hope here was to have the emission from a reporter group change with binding and dissociation without perturbing the interaction kinetics. One site of cysteine substitution was at R92 adjacent to the inhibitory pseudosubstrate sequence and the other at R239 in the C helix (Figure 1B and C).

With the FM-R92C conjugate, it was possible to measure the association and dissociation rate constants for C binding in the absence and presence of cAMP; however, it was not possible to measure this with the FM-R239C conjugate. Cyclic-AMP was found to selectively accelerate the rate of RIα (91−244):C dissociation by 700-fold without affecting the association rate. Additionally, the rate of RIα (91−244):C-subunit dissociation was unaffected by excess PKI(5−24), indicating that PKI(5−24) simply binds to the dissociated C subunit and prevents reassociation of the C subunit with RIα (91−244). This strongly suggests that small pseudosubstrates and presumably, at least, small substrates do not bind directly to the RIα (91−244):C complex and supports a mechanism for substrate-facilitated cAMP-induced dissociation that involves a mass action effect of excess substrate and not direct substrate binding to holoenzyme.

EXPERIMENTAL PROCEDURES

Materials. Protein kinase-A inhibitor fragment 5−24 amide trifluoroacetate salt (PKI(5−24)) was obtained from Sigma-Aldrich Corp. (St. Louis). All other chemicals were at least regent grade.

Preparation of the RIα (91−244) Mutants. Two cysteine substitution mutants (R92C and R239C) of RIα (91−244) subunit were prepared as described previously (*12*).

Fluorescein Maleimide Labeling. The R-subunit samples (12.5−25 nmol) were initially buffer exchanged by elution through a G-25 column (1.5 × 7 cm) equilibrated with buffer (50 mM MOPS at pH 7.0 with 50 mM NaCl). The protein fractions were pooled, and the concentrations of the pooled samples were determined with the Bradford assay (*13*). The protein concentrations of the reaction mixtures ranged between 3 and 6 μM. Labeling reactions with fluorescein maleimide were allowed to proceed for 1 h at room temperature, protected from light, and then eluted through a Sephadex G-25 column (2.5 × 6 cm) equilibrated with buffer (50 mM MOPS at pH 7.0, with 50 mM NaCl, and 1 mM DTT) at room temperature. Fluorescein emission (excitation at 470 nm and emission at 525 nm) from the column fractions was measured, and the fluorescent fractions with retention times that corresponded to the unmodified R subunit were pooled. Aliquots of the pooled fractions were subjected to gel electrophoresis under denaturing conditions (12% SDS−PAGE), and the fluorescent bands were visualized with a mineral lamp to assess whether any unconjugated fluorescein was associated with the R mutants.

Phosphotransferase Assay. The activity of the labeled R mutants was evaluated by assessing its ability to inhibit the phosphotransferase activity of recombinant C subunit using the method of Cook et al. with kemptide (LRRASLG) as a substrate (*14*).

Determination of the Stoichiometry of Labeling. The stoichiometry of FM-labeled R was determined spectrophotometrically by substitution of the measured absorbance values at 497 nm (A_{497}) and the protein concentration [R] determined with the Bradford assay (*13*) into the following expression:

$$[\text{Fluorescein}]/[\text{R}] = (A_{497}/83\,000)/[\text{R}] \qquad (1)$$

Removal of cAMP from RIα (91−244). One milliliter of cAMP-agarose 6% (Sigma-Aldrich Corp., St. Louis; catalog no. A-7775) that had been equilibrated with buffer (50 mM MOPS at pH 7.0 with 50 mM NaCl and 1 mM DTT) was combined with 2 mL of labeled protein (2−4 μM) and incubated overnight at 4 °C. In the morning, the excess buffer was aspirated off, and the resin was washed twice with buffer at room temperature. (Note that the cAMP-agarose 6% has been discontinued and that cAMP-agarose lyophilized powder, catalog number A0144, from Sigma-Aldrich Corp. is a functionally equivalent product in our hands.) The FM-labeled R subunit was released from the resin by incubation of the protein/resin complex for 0.5 h at room temperature with buffer (20 mM MES at pH 5.8 with 100 mM NaCl)

that included cGMP (25 mM). The released protein was then dialyzed overnight at 4 °C against 3 × 1 L changes in buffer (50 mM MOPS at pH 7.0 with 50 mM NaCl and 1 mM DTT).

Formation of RIα (91−244):C Complexes. The labeled R mutants (1 μM) were combined with a 1.2-fold molar excess of recombinant C and then dialyzed (cutoff = 30 kDa) overnight at 4 °C against 3 × 1 L changes in 50 mM MOPS at pH 7.0 with 50 mM NaCl, 1 mM DTT, 2 mM $MgCl_2$, and 0.2 mM ATP. Free C and R subunits were separated from the RIα (91−244):C complexes by elution through a Sephacryl S-75 column (1.5 × 25 cm) using buffer (50 mM MOPS at pH 7.0 with 50 mM NaCl, 2 mM $MgCl_2$, 0.2 mM ATP, and 1 mM DTT).

Steady-State Emission Spectra. Steady-state emission spectra were measured at room temperature using an Instrument S. A., Inc. Jobin Yvon/Spex FluoroMax II spectrofluorometer with the excitation and emission band widths set at 5 nm. All spectrofluorometric measurements were performed with samples suspended in 50 mM MOPS at pH 7.0 with 50 mM NaCl, 1 mM DTT, 2 mM $MgCl_2$, and 0.2 mM ATP.

Time-Resolved Fluorescence Anisotropy. Emission anisotropy was determined as previously described (*15*). Unless stated otherwise, emission anisotropy decay was analyzed with the impulse reconvolution method implemented in the DAS6 software package from HORIBA Jobin Yvon IBH Ltd. (Glasgow, U.K.) described elsewhere (*16*). Briefly and simply, this approach splits the analysis into two steps: analysis of the total emission decay, $S(t)$, from the vertically, $I_{||}(t)$, and orthogonally, $I_{\perp}(t)$, polarized emission components, followed by analysis of the vertical/perpendicular difference emission decay, $D(t)$. $S(t)$, free of anisotropy effects, is given by the expression

$$S(t) = I_{||}(t) + G \cdot 2I_{\perp}(t) \quad (2)$$

and is analyzed as a biexponential function. G is a measure of the instrumental polarization bias (0.995). $D(t)$, which includes both fluorescence and anisotropy parameters, is given by the following expression:

$$D(t) = I_{||}(t) - G \cdot I_{\perp}(t) \quad (3)$$

$D(t)$ is deconvolved with the results from the $S(t)$ analysis as a constraint yielding the following:

$$r(t) = \beta_1 \exp(-t/\phi_1) + \beta_2 \exp(-t/\phi_2) \quad (4)$$

Here, β_1 and β_2 are the amplitudes of the anisotropy at time zero for the fast and slow anisotropy decay processes, respectively. ϕ_1 and ϕ_2 are the fast and slow rotational correlation times of the anisotropy decay, respectively. ϕ_2 usually yields an estimate of the whole-body rotational correlation time when it is less than about five times the emission lifetime and when the rate of the segmental motions around the site of reporter group conjugation greatly differ from the rate of the whole-body diffusion. A nonassociative model was assumed, where the emission relaxation times are common to all of the rotational correlation times. Goodness of fit was evaluated from the values of the reduced χ^2_r and by visual inspection of the weighted residual plots. All time-resolved anisotropy measurements were performed with samples suspended in 50 mM MOPS at pH 7.0 with 50 mM NaCl, 1 mM DTT, 2 mM $MgCl_2$, and 0.2 mM ATP at 22 °C.

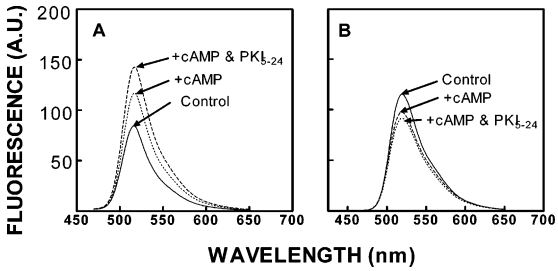

FIGURE 2: Effect of cAMP and PKI(5−24) on emission spectra of FM-RIα (91−244):C-subunit complexes. Fluorescence spectrum with excitation at 470 nm of the RIα (91−244):C complex labeled with fluorescein maleimide at R92C (panel A) and R239C (panel B) in the holoenzyme state (solid line) (100 nM) and following the addition of first cAMP (10 μM) (···) and then PKI(5−24) (10 μM) (---). Measurements were made with the samples suspended in 50 mM MOPS at pH 7.0, with 50 mM NaCl, 1 mM DTT, 0.2 mM ATP, and 2 mM $MgCl_2$ at room temperature.

Stopped-Flow Kinetic Measurements. Stopped-flow experiments were conducted with an Applied Photophysics SX.18MV (Leatherhead, U.K.) stopped-flow spectrofluorometer. The FM conjugates were excited at 460 nm, and an Omega interference filter (510DF23) was used to select the fluorescence signal. The second-order association rate constants for the binding of C subunit to the RIα (91−244) conjugates were determined from the slope of plots of the observed rate of fluorescence change versus final C-subunit concentration. The first-order rate constant of R−C dissociation was determined by mixing the preformed FM-labeled RIα (91−244) complexes with unlabeled RIα (91−244) in large excess and fitting the tracings to a single-exponential equation. All samples were suspended in buffer containing 50 mM MOPS at pH 7.0 with 50 mM NaCl, 1 mM DTT, 2 mM $MgCl_2$, and 0.2 mM ATP. Equilibrium dissociation constants (K_d) were determined as a ratio of the dissociation to association rate constants.

RESULTS

Preparation, Labeling, and Characterization of the RIα (91−244) Mutants. The two cysteine substitution mutants were overexpressed and purified to greater than 95% as assessed by a visual inspection of the Coomassie-stained SDS−PAGE gel and FPLC profiles. The mass spectroscopy of each mutant was consistent with the expected fragmentation masses of the desired mutant (data not shown). Both cysteine substitution mutants were equally as effective as RIα (91−244) at inhibiting the phosphotransferase activity of the wild-type C subunit (data not shown). Denaturing SDS−PAGE analysis of the fluorescein conjugates showed no detectable nonconjugated probe, and the stoichiometry of fluorescein conjugation was ∼28% and ∼40% for the FM-R92C-RIα (91−244) and FM-R239C-RIα (91−244) conjugates, respectively.

Effects of cAMP and PKI(5−24) on Labeled Holoenzyme Emission Spectra. The emission spectra of the FPLC purified FM-R92C-RIα (91−244) and FM-R239C-RIα (91−244) mutants complexed to the C subunit in the absence and presence of cAMP or cAMP plus PKI(5−24) are illustrated in Figure 2. Although the emission intensities changed in a

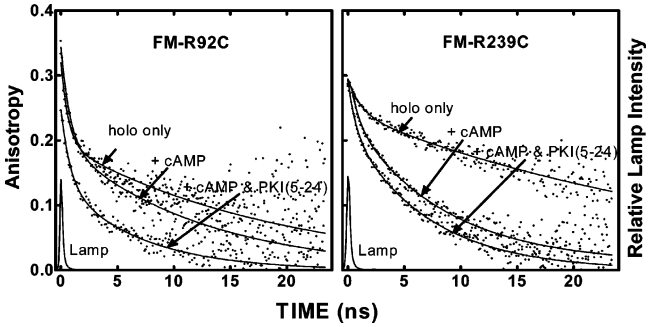

FIGURE 3: Effect of cAMP and PKI(5−24) on the time-resolved anisotropy decay of the FM-RIα (91−244):C Subunit complexes. (Left panel) FM-R92C-RIα (91−244):C complex (100 nM). (Right panel) FM-R239C-RIα (91−244):C complex (100 nM). Data were accumulated initially in the absence of ligands, followed by the addition of cAMP (25 μM) and then by the addition of PKI(5−24) (10 μM). The smooth line through each decay plot was generated with best fit parameters for a biexponential (eq 4). Measurements were made with the samples suspended in 50 mM MOPS at pH 7.0 with 50 mM NaCl, 1 mM DTT, 0.2 mM ATP, and 2 mM $MgCl_2$ at 22 °C.

mutant-dependent manner, the emission maxima of the FM-R92C and FM-R239C conjugates did not change with the addition of cAMP or the subsequent addition of PKI(5−24) and were 516 and 519 nm, respectively (Figure 2). In the case of the FM-R92C conjugate, the addition of cAMP increased the emission intensity ∼37% and a further ∼24% with the subsequent addition of PKI(5−24) (Figure 2A). In the case of the FM-R239C conjugate, the addition of cAMP was associated with about a 16% decrease in emission intensity followed by a further ∼5% decrease with the subsequent addition of PKI(5−24) (Figure 2B). These changes in emission intensity are reflective of the differential microenvironments of the reporter groups and the inability of cAMP alone to induce complete holoenzyme dissociation under these conditions. This latter conclusion is consistent with the previous report of the limited ability of cAMP to induce type I holoenzyme dissociation under equilibrium conditions (*17*). This conclusion is also supported by the time-resolved fluorescence anisotropy data from these samples that show that the addition of only cAMP is not associated with the slow (φ_2) and presumably whole-body rotational correlations times of the free FM-RIα (91−244) mutants. Specifically, in the holoenzyme state, the φ_2 values of the FM-R92C:C-subunit and the FM-R239C:C-subunit complexes were observed to be 38.3 ± 9.6 ns ($n = 3$) and 35.5 ± 5.1 ns ($n = 9$), respectively (Figure 3and Table 1). These values are reasonably close to what would be predicted by the Stokes−Einstein equation (23.9 ns) for the holoenzyme (M_r equal to ∼57,000) given the short lifetime of the reporter group (∼4 ns). Addition of only cAMP reduced the φ_2 values of the FM-R92C and FM-R239C conjugates to 17.5 ± 0.9 ns ($n = 3$) and 10.0 ± 1.6 ns ($n = 3$), respectively (Table 1). These values are greater than what is observed for completely dissociated holoenzymes because the addition of cAMP plus PKI(5−24), which induces complete dissociation of the holoenzyme, reduced the rotational correlation times for the FM-R92C and FM-R239C holoenzymes to 8.8 ± 2.3 and 7.1 ± 0.1 ns ($n = 3$), respectively (Table 1). These values are again approximately those predicted by the Stokes−Einstein equation (7.4 ns) for spherical proteins the size of the RIα (91−244) conjugates (M_r equal ∼17,700).

Kinetics of C Binding to RIα (91−244). Because emission intensity from both labeled conjugates changed with C binding (albeit the emission from the FM-R92C mutant decreased ∼40% and the FM-R239C mutant increased ∼20%), we measured the binding kinetics of both mutants with stopped-flow spectrofluorometry. Representative stopped-flow tracings associated with the rapid mixing of FM-R92C and the FM-R239C conjugates with various concentrations of C are illustrated in Figures 4A and 5A, respectively. The bimolecular association rate constants determined from the slopes of plots of the observed rate constant for fluorescence change versus final the concentration of the C subunit are illustrated in the insets. (Please note that the phrase observed rate constants is used here and below with the understanding that the measurements are made under first-order conditions so the observed rate of change of fluorescence can be treated as constant for the reaction.) The measured association rate constants for both conjugates were within experimental error of each other (∼2.4×10^7 $M^{-1}s^{-1}$; Table 2). The dissociation rate constants were determined from fitting the fluorescence tracings associated with the rapid mixing of preformed complexes of the C subunit and FM-R92C or FM-R239C conjugates with excess unlabeled RIα (91−244) to a single-exponential equation. Representative tracings using 1 μM unlabeled RIα (91−244) are illustrated in Figures 4B and 5B. The averaged dissociation rate constants for FM-R92C and FM-R239C mutants were within a factor of 2 of each other ($3.7 \pm 1.0 \times 10^{-3}$ and $6.9 \pm 0.2 \times 10^{-3}$ s^{-1}, respectively (Table 2)). Dissociation measurement with 1, 2, or 4 μM PKI(5−24) alone or 1 μM PKI(5−24) plus 5 μM α4 integrin tail (an A-kinase substrate) yielded essentially the same results (data discussed in more detail below), supporting the unimolecular character of this reaction and the validity of these k_{-1} values.

Dividing the dissociation by the association rate constants for the R92C and R239C mutants yielded K_d values of 0.15 and 0.28 nM, respectively, which from an experimental point of view are essentially the same and remarkably close to the published values for C subunit binding to wild-type RIα and a Δ1−91 RIα deletion mutant: 0.39 and 0.23 nM, respectively (*9*).

cAMP Effects on RIα (91−244):C Binding Kinetics. Encouraged by the capacity of both FM-labeled conjugates to monitor the C-subunit binding kinetics, we examined the effect of cAMP on C subunit binding of both mutants; however, only the FM-R92C conjugate yielded unambiguous results. Representative stopped-flow tracings associated with the rapid mixing of FM-R92C and the FM-R239C conjugates with various concentrations of C subunit in the presence of cAMP (10 μM) are illustrated in Figures 6A and 7A, respectively. The fluorescence tracings associated with the rapid mixing of the FM-R92C conjugate with the C subunit were well fit to a single-exponential equation, and the bimolecular association rate constant was determined from the slope of the plot of the observed rate constants for fluorescence change versus the final concentration of the C subunit (Figure 6A, inset). The value of the association rate constant was essentially identical to that determined in the absence of cAMP (2.3×10^7 $M^{-1}s^{-1}$; Table 2), indicating that cAMP binding to RIα (91−244) does not affect the association process. The time course of dissociation of the FM-R92C:C-subunit conjugate complex, however, was dra-

Table 1: Effect of cAMP and PKI(5−24) on the Time-Resolved Anisotropy Decay Parameters of the FM-Labeled RIα (91−244):C Subunit Complexes

conjugate	added ligands	β_1[a]	β_2[b]	ϕ_1[c] (ns)	ϕ_2[d] (ns)	ψ^2_r[e]
FM-R92C-RIα (91−244)	alone	0.075 ± 0.020	0.161 ± 0.015	03.66 ± 0.6	38.0 ± 1.5	1.6 ± 0.1
FM-R92C-RIα (91−244)	cAMP	0.109 ± 0.012	0.140 ± 0.035	1.9.0 ± 0.4	17.5 ± 0.9	1.2 ± 0.1
FM-R92C-RIα (91−244)	cAMP and PKI(5−24)	0.089 ± 0.006	0.110 ± 0.008	1.0 ± 0.3	8.8 ± 2.3	1.6 ± 0.2
FM-R239C-RIα (91−244)	alone	0.34 ± 0.005	0.220 ± 0.013	2.5 ± 0.8	35.5 ± 5.1	1.3 ± 0.1
FM-R239C-RIα (91−244)	cAMP	0.105 ± 0.045	0.145 ± 0.059	2.6 ± 01.4	10.0 ± 0.5	1.6 ± 0.1
FM-R239C-RIα (91−244)	cAMP and PKI(5−24)bound	0.047 ± 0.009	0.189 ± 0.012	1.5 ± 0.3	7.1 ± 0.1	1.8 ± 0.2

[a] Amplitude of the fast anisotropy decay processes. [b] Amplitude of the slow anisotropy decay processes. [c] Rotational correlation time of fast anisotropy decay processes. [d] Rotational correlation time of slow anisotropy decay processes. [e] Reduced ψ_r^2 of the anisotropy decay analysis

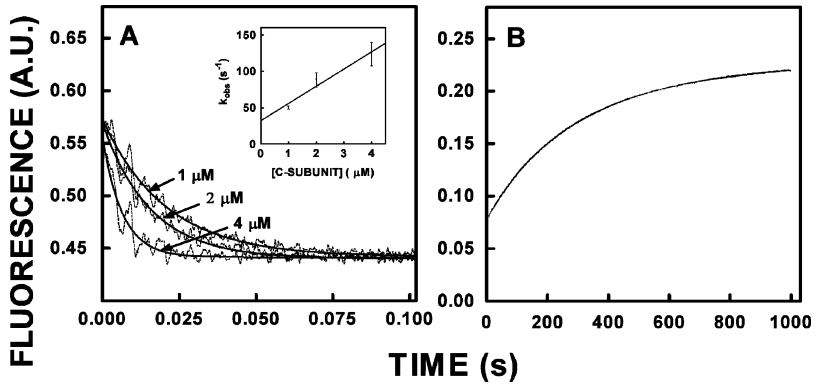

FIGURE 4: Stopped-flow kinetics of FM-R92C-RIα (91−244) binding to and dissociating from the C subunit in the absence of cAMP. (Panel A) Stopped-flow traces of FM-R92C-RIα (91−244) rapidly mixed with the C subunit in the absence of cAMP. The final concentration of FM-RIα (91−244) R92C was 100 nM, and the concentration of the C subunit was varied from 1 to 4 μM. The decreasing emission follows the time course of binding. The solid lines denote the best fit of the data to a single-exponential equation. The inset shows the plot of observed mean ± SD ($n = 3$) rates of change of fluorescence (observed rate) vs C-subunit concentration. (Panel B) Stopped-flow trace of the rapidly mixed FM-R92C-RIα (91−244):C-subunit complex (100 nM) with excess unlabeled R92C-RIα (91−244) (1 μM). The increasing emission signal follows the time course of the replacement of the FM-R92C mutant with the unlabeled RIα mutant. Samples were suspended in a buffer containing 50 mM MOPS at pH 7.0, 50 mM NaCl, 1 mM DTT, 2 mM $MgCl_2$, and 0.2 mM ATP at 22 °C.

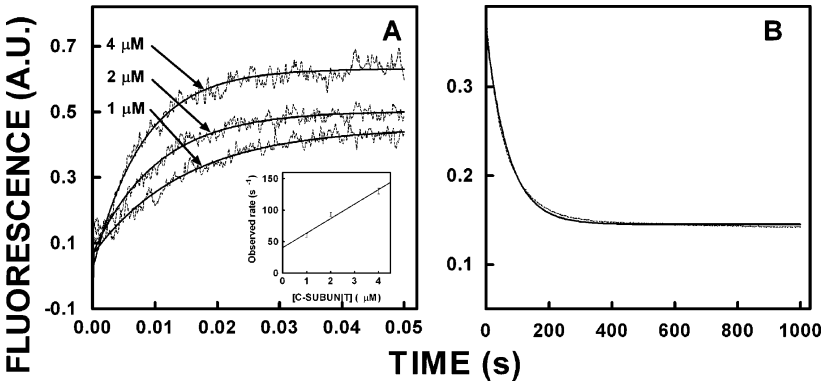

FIGURE 5: Stopped-flow kinetics of FM-R239C-RIα (91−244) binding to and dissociating from the C subunit in the absence of cAMP. (Panel A) Stopped-flow traces of FM-R239C-RIα (91−244) rapidly mixed with the C subunit in the absence of cAMP. The final concentration of FM-R239c-RIα (91−244) was 100 nM, and the concentration of the C subunit was varied from 1 to 4 μM. The increasing emission follows the time course of binding. The solid lines represent the best fit of the data to a single-exponential equation. The inset shows the plot of observed mean ± SD ($n = 3$) rates of change of fluorescence (observed rate) vs C-subunit concentration. (Panel B) Stopped-flow trace of the rapidly mixed FM-R239C-RIα (91−244):C-subunit complex (100 nM) with excess unlabeled RIα (91−244) R239C (1 μM). The decreasing emission signal follows the time course of the replacement of the FM-R239C mutant with the unlabeled R239C-RIα mutant. Please see the legend to Figure 4 for additional details.

matically affected by cAMP. Figure 6B illustrates a representative stopped-flow tracing associated with the rapid mixing of preformed FM-R92C:C-subunit complexes (100 nM) and excess unlabeled RIα (91−244) (1 μM). Fitting the experimental tracings to a single-exponential equation yielded a unimolecular dissociation rate constant of 2.6 s^{-1}, ~700-fold faster than that in the presence of cAMP (Table 2). (Additionally, a similar value for the dissociation rate constant (2.8 ± 0.8 s^{-1}, $n = 10$) was observed by monitoring cAMP-induced (100−1000 μM) dissociation of FM-R92C:C-subunit complexes (data not shown), which again supports the unimolecular character of this reaction and the validity of these k_{-1} values.) Dividing the dissociation by the association rate constants yielded a K_d value of 130 nM, again ~700-fold higher than what we observed in the absence of cAMP.

In the case of the FM-R239C conjugate, the C-subunit binding tracings were not only noisier because of the much

Table 2: Effect of cAMP on the Association and Dissociation Rate Constants for C-Subunit Binding to FM-Labeled RIα (91−244) Mutants

condition	k_1[a] ($M^{-1}s^{-1}$)	k_{-1}[b] (s^{-1})	K_D[c] (nM)
FM-R92C-RIα (91−244) (w/o cAMP)	$2.4 \pm 0.5 \times 10^7$	$3.7 \pm 0.1 \times 10^{-3}$	0.15
FM-R92C-RIα (91−244) (w/ cAMP)	$2.0 \pm 0.3 \times 10^7$	2.6 ± 0.5	130
FM-R239C-RIα (91−244) (w/o cAMP)	$2.5 \pm 0.3 \times 10^7$	$6.9 \pm 0.2 \times 10^{-3}$	0.28
FM-R239C-RIα (91−244) (w/ cAMP)	n.d.	5.3 ± 0.9	

[a] Bimolecular association rate constants determined from the rapid mixing of FM-labeled RIα (91−244) mutants (100 nM) with various concentrations of the C-subunit in the absence and presence of cAMP (10 μM) under pseudo-first-order conditions ($n = 4$). [b] Unimolecular dissociation rate constants determine by rapidly mixing excess unlabeled RIα (91−244) with the preformed RIα (91−244):C complex (100 nM) of FM-labeled RIα (91−244) conjugates and the C-subunit in the absence and presence of cAMP (10 μM) ($n = 3$). [c] Equilibrium dissociation constants determined by dividing the unimolecular dissociation constant by the bimolecular association rate constants.

smaller change in fluorescence (~5%) but also the emission intensity initially decreased then increased, rendering simple single-exponential analysis impossible (Figure 7A). The molecular basis for this complex time course of emission is unclear, but it most likely represents an initial binding-dependent decrease in emission followed by multiple slow conformational changes that are associated with increased emission. The tracings generated to measure the rate of dissociation of the cAMP-bound FM-R239C:C-subunit complex were also very noisy but could be fit to a single-exponential equation, albeit without the same level of accuracy for the fitting parameters. Figure 7B illustrates a stopped-flow tracing associated with the rapid mixing of preformed FM-R239C:C-subunit complexes (100 nM) and excess unlabeled RIα (91−244) (1 μM). Fitting the experimental tracings to a single-exponential equation yielded a unimolecular dissociation rate constant of 5.3 s^{-1}, which is within a factor of 2 of what we observed with the FM-R92C mutant (Table 2). Because of the low signal-to-noise ratio and the complexity of the binding tracings associated with the FM-R239C conjugate, only results with the FM-R92C conjugate were used in the final quantification of the RIα (91−244):C-subunit binding kinetics and in the assessment of the effects of PKI(5−24) on RIα (91−244):C-subunit binding.

PKI(5−24) Effects on RIα (91−244):C-Subunit Dissociation Kinetics. To better understand the interaction of substrate and cAMP in the activation of type-I A-kinase, we examined the possibility that substrate enhancement of type-I A-kinase activation is achieved through a direct interaction with the holoenzyme complex. This could occur if the pseudosubstrate inhibitor domain of the R subunit, on its own, mediated weak interactions with the active site of the C subunit, leaving the active site transiently unoccupied for substrate binding. This appears plausible because the reporter group, conjugated to the R92C residue and adjacent to the pseudosubstrate inhibitory domain, is highly flexible when complexed to the C subunit, on the basis of an analysis of the time-resolved anisotropy decay of the FM-R92C:C-subunit complex (Figure 3). Consequently, we examined the possibility of a pseudosubstrate binding directly to the FM-R92C:C subunit forming a ternary complex. We reasoned that if the substrate binds to the holoenzyme at one of the C−R binding surfaces, that is, a consensus sequence binding surface, or at an allosteric control site that affects C−R binding kinetics, then the affinity of the subunits toward each other would be reduced, and excess substrate would, in a concentration-dependent manner, accelerate the apparent rate of dissociation. To test this idea, we measured the effect of various excess concentrations of PKI(5−24) on the rate of dissociation of FM-R92C:C-subunit complexes. Here, as with the rapid mixing of excess unlabeled RIα (91−244) described in the earlier section, PKI(5−24) should minimally bind to the dissociated FM-R92C conjugate and be observed as a time-dependent increase in emission intensity. If there were direct binding of PKI(5−24) to holoenzyme, one would observe zero-order dissociation plus either first- or second-order dissociation depending upon the reaction conditions. Figure 8 illustrates representative traces produced by the rapid mixing of FM-R92C:C-subunit complexes (100 nM) with various concentrations of PKI(5−24) (1, 2, and 4 μM). The observed rate constants were determined by fitting the traces to a single-exponential equation and then plotting as a function of the final concentration of PKI(5−24) (Figure 8, inset). The averaged observed rate constant of dissociation varied little with PKI(5−24) concentration, indicating that it does not bind directly to the complex to facilitate dissociation. The mean (±SD) observed rate of dissociation for all of the samples was $3.7 \pm 0.4 \times 10^{-3}$ s^{-1}, a value that is within experimental error of that observed with excess RIα (91−244) as a replacing agent (Table 2).

Kemptide, Ala-Kemptide, and α4-Integrin Cytoplasmic Domain Effects on RIα (91−244):C-Subunit Dissociation Kinetics. To begin to assesses whether the above results could be generalized to substrates, we initially examined the effect of a small substrate, kemptide, on the dissociation of the FM-RIα (91−244):C-subunit complex, and the results are shown in Figure 9A. Kemptide, even at a final concentration of 500 μM, had a limited capacity to dissociate the FM-RIα (91−244):C-subunit complex. Kemptide initially induced holoenzyme dissociation, albeit with magnitude and rate in comparison to that produced by PKI(5−24) (Figure 9A). This was followed by a slow decrease in fluorescence, suggesting reassociation of the holoenzyme. Believing that this behavior was due to the phosphorylation of kemptide and subsequent dissociation of the lower affinity phospho-kemptide:C-subunit complex, we repeated this experiment with Ala-kemptide (LRRAALG), which has an Ala at the P-site and cannot be phosphorylated. The results with Ala-kemptide are illustrated in Figure 9B and show that rapid mixing of 500 μM Ala-kemptide was associated with essentially the same rate of dissociation produced by excess PKI(5−24) (1 μM), confirming that substrate phosphorylation limited the capacity of kemptide to dissociate holoenzyme.

Postulating that large substrates might bind directly to the holoenzyme to accelerate the dissociation of the R and C subunits, we compared the effect of PKI(5−24) alone with a combination of PKI(5−24) plus α4-integrin cytoplasmic domain, a A-kinase substrate (*18*), on the rate of dissociation of FM-RIα (91−244):C-subunit complexes. The results of this experiment are illustrated in Figure 9C and show that the presence of α4-integrin cytoplasmic domain had no added

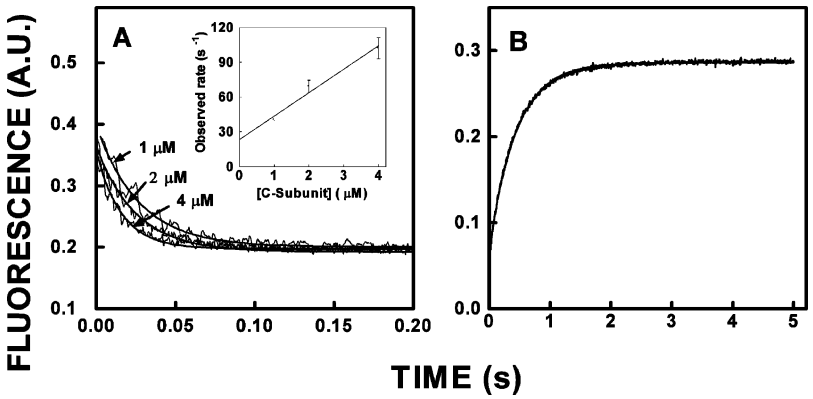

FIGURE 6: Stopped-flow kinetics of FM-R92C-RIα (91−244) binding to and dissociating from the C subunit in the presence of cAMP. (Panel A) Stopped-flow traces of FM-R92C-RIα (91−244) rapidly mixed with the C subunit in the presence of cAMP (10 μM). (Panel B) Stopped-flow trace of the rapidly mixed FM-R239C-RIα (91−244):C-subunit complex (100 nM) with excess unlabeled RIα (91−244) R239C (1 μM) in the presence of cAMP (10 μM). Please see the legend to Figure 4 for additional details.

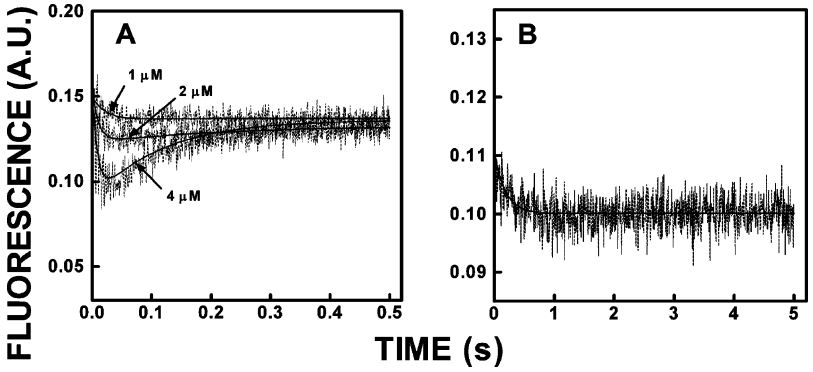

FIGURE 7: Stopped-flow kinetics of FM-R239C-RIα (91−244) binding to and dissociating from the C subunit in the presence of cAMP. (Panel A) Stopped-flow traces of FM-R239C-RIα (91−244) rapidly mixed with the C subunit in the presence of cAMP (10 μM). The final concentration of FM-R239c-RIα (91−244) was 100 nM, and the concentration of the C subunit was varied from 1 to 4 μM. (Panel B) Stopped-flow trace of the rapidly mixed FM-R239C-RIα (91−244):C-subunit complex (100 nM) with excess unlabeled RIα (91−244) R239C (1 μM) in the presence of cAMP (10 μM). Please see the legend to Figure 4 for details.

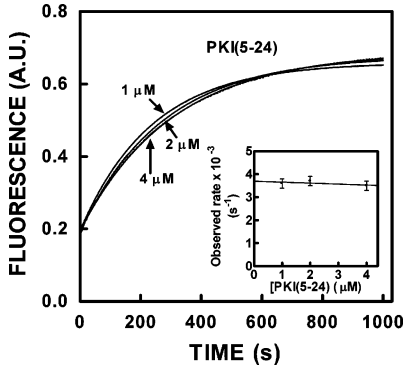

FIGURE 8: Effect of PKI(5−24) on the dissociation of FM-R92C-RIα (91−244):C-subunit complexes. Stopped-flow traces of FM-R92C-RIα (91−244):C-subunit complexes (100 nM final concentration) rapidly mixed with 1, 2, and 4 μM (final concentrations) PKI(5−24). The increasing emission follows the time course of dissociation of the R−C complexes and binding of PKI(5−24) to the free C subunit. The solid lines represent the best fit of the data to a single-exponential equation. The inset shows a plot of observed rates of fluorescence change (observed rate) vs the final concentration of PKI(5−24) ($n = 3$). Please see the legend to Figure 4 for additional details.

effect on PKI(5−24)-induced dissociation of FM-RIα (91−244):C-subunit complexes, which is consistent with a simple competitive displacement mechanism for substrate-induced dissociation of the A-kinase holoenzyme.

DISCUSSION

In the biological sciences, it is almost a truism that cAMP induces the dissociation and subsequent activation of the A-kinase holoenzyme. The basis for this belief rests upon three plus decade old observations with ultracentrifugation (*19*, *20*), gel filtration (*21*), and ion-exchange chromatography (*22*, *23*) that showed micromolar concentrations of cAMP produced dissociation of the holoenzyme into an R dimer and two C subunits. The chromatographic procedures demonstrating the actions of cAMP primarily utilized forces of dilution to separate the less tightly bound R and C subunits but provided little quantitative information on the magnitude of cAMP-induced changes in R−C affinity. This report describes the development and use of a method to measure the binding rate constants and affinity of RIα (91−244) and C subunits toward each other. With this approach, we generated a quantitative and more mechanistic understanding of cAMP-induced activation of type I A-kinase, finding that cAMP acts by dramatically accelerating the rate of dissociation of RIα from the C subunit by 700-fold without affecting the association kinetics. Despite the resulting 700-fold reduction in affinity, the K_d of RIα toward the C subunit is still substantial (130 nM) and readily explains why cAMP does not induce complete type-I A-kinase holoenzyme dissociation at low micromolar concentrations and in the absence of dilution forces (*17*).

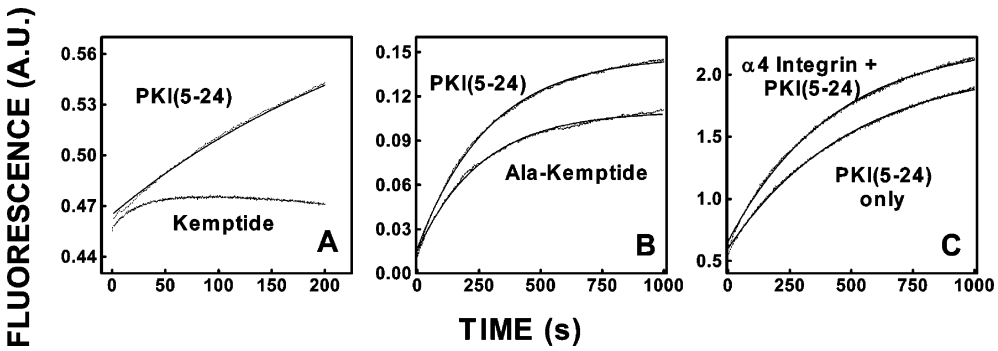

FIGURE 9: Effect of kemptide, Ala-kemptide, and α4 Integrin Tail Plus PKI(5−24) on the dissociation of FM-R92C-RIα (91−244):C-subunit complexes. Shown are stopped-flow traces of FM-R92C-RIα (91−244):C-subunit complexes (100 nM) rapidly mixed with kemptide (500 μM) (panel A), Ala-kemptide (500 μM) (panel B), or a mixture of α4 integrin cytosolic domain (5 μM) and PKI(5−24) (1 μM) (panel C). The increasing emission follows the time course of dissociation of the R−C complexes and the binding of the competing ligand to free the C subunit. Note that kemptide becomes phosphorylated and that the phosphorylated kemptide binds with lower affinity to the C subunit and is consequently associated with reassociation of the R−C complexes. Also note that only post-mixing concentrations are indicated and that the *y*-axes differ because the photomultiplier (PMT) voltage was set at different values for the samples illustrated in each panel. (The PMT voltage affects apparent fluorescence intensity but not observed rates.) Finally, note that the difference in the rates of change of fluorescence (∼40%) between the results in panels B and C represent prep-to-prep differences measured 1 year apart. The solid lines represent the best fit of the data to a single-exponential equation. For comparison, each plot includes a control plot of the effect of PKI-(5−24) (1 μM) on the dissociation of FM-R92C-RIα (91−244):C subunit preformed on the same day and instrument settings as the sample of interest. Please see the legend to Figure 4 for additional details.

To our knowledge, there have been only two other reports of the affinity of the C and RIα subunits toward each other in the presence of cAMP. One was from our laboratory, where the K_d value was reported to be 11 nM using surface plasmon resonance (*9*); however, this value is problematic for two reasons: First, the C subunit was immobilized on the Biacore chip, and the dimeric wild-type RIα was in the mobile phase, yielding approximate estimates of the binding rate constants because each monomer of dimeric R could not bind the C subunit with equal probability. Second, and more importantly, the measurements were made with cAMP-bound RIα complexes and not in the presence of excess cAMP. Consequently, both free and cAMP-bound RIα were in the mobile phase, which would elevate the apparent affinity. The other report was by Doskeland and his associates (*24*) who used equilibrium approaches to determine the K_d of R−C binding in the presence of cAMP to be 160−240 nM, a value comparable to the value reported here (130 nM); however, the rate constants could not be assessed with their approach.

In addition to determining the rate constants for R−C binding, we examined the possibility that substrates bind directly to the holoenzyme and act either sterically or allosterically to facilitate holoenzyme dissociation. Initially, using PKI(5−24) to mimic the effects of substrate, the rate of dissociation of FM-R92C:C subunit complex was not influenced by excess PKI(5−24). This experiment was followed by one in which both excess PKI(5−24) and a large substrate, α4 integrin cytosolic domain, were rapidly mixed with the FM-RIα (91−244):C-subunit complex, and no enhanced holoenzyme dissociation was observed. All this argues for a simple mechanism for substrate-facilitated cAMP-induced dissociation, that is, the replacement of R subunits through a mass action effect of excess substrate. A simplified reaction mechanism for this process is illustrated in Scheme 1, where S represents the substrate and P the product. In this light, cAMP regulation of the A-kinase should be viewed as a dynamic process wherein each of the molecular components binds with probabilities governed by their concentrations.

Scheme 1

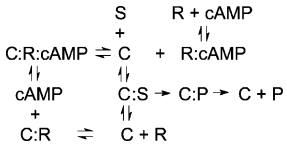

Although the present work represents an *in vitro* analysis of cAMP and pseudosubstrate on R−C binding kinetics, it has ramifications for *in vivo* cAMP regulation of A-kinase activity. Specifically, the present work helps explain why in cells cAMP induces the complete dissociation of type-II A-kinase holoenzyme but not type-I (*25*). At low micromolar concentrations of A-kinase estimated in subcellular compartments (*26*), cAMP binding does not sufficiently lower the affinity of the RIα and C subunits toward each other to allow complete dissociation. The presence of substrate can enhance dissociation, but as we observed with kemptide (Figure 9A), substrates are rapidly phosphorylated. Phosphorylated substrates bind the C subunit with a lower affinity, increasing the probability of the dissociation of phosphorylated substrate: C-subunit complexes and subsequent reassociation of the freed C subunit with RIα subunits. The type-II R subunits, however, are autophosphorylated in the presence of cAMP and MgATP, and phospho-RII binds the C subunit with about an order of magnitude lower affinity (*27*), greatly increasing the *in vivo* probability of cAMP-induced dissociation in the presence of the typically high intracellular concentrations of MgATP.

Three final comments: First, in two older studies of ours (*28*, *29*), cAMP in the presence of MgATP was not observed to induce the complete dissociation of type-II holoenzyme. In these studies, the samples were nonspecifically labeled with amine-reactive probes that may have blocked the effect of autophosphorylation on the R−C binding affinity and prevented complete dissociation. Second, although the FM-R92C conjugate is clearly better suited for R−C binding kinetics studies, the FM-R239C conjugate can be used to measure the association kinetics of cAMP binding to R−C complexes. With the FM-R239C conjugate, we determined

the association rate constant for cAMP binding to the FM-R239C:C-subunit complex to be $3.1 \times 10^6\ M^{-1}s^{-1}$ (data not shown). Third, in our measurement of the association rate constants (Figures 4−6), we utilized a narrow range of C-subunit concentrations so that a two or more step binding mechanism cannot be excluded.

ACKNOWLEDGMENT

We thank Choel Kim for helping us select the sites of cysteine substitution and conjugation and Laura Ellis for help with protein purification. In addition, we thank Drs. Mark Ginsberg and James Lim for providing the α4-integrin cytoplasmic domain.

REFERENCES

1. Colledge, M., and Scott, J. D. (1999) AKAPs: from structure to function, *Trends Cell Biol. 6*, 216−221.
2. Taylor, S. S., Kim, C., Vigil, D., Haste, N. M., Yang, J., Wu, J., and Anand, G. S. (2005) Dynamics of signaling by PKA, *Biochim. Biophys. Acta 1754*, 25−37.
3. Huang, L. J., and Taylor, S. S. (1998) Dissecting cAMP binding domain A in the RIalpha subunit of cAMP-dependent protein kinase. Distinct subsites for recognition of cAMP and the catalytic subunit, *J. Biol. Chem. 273*, 26739−26746.
4. Ringheim, G. E., and Taylor, S. S. (1990) Effects of cAMP-binding site mutations on intradomain cross-communication in the regulatory subunit of cAMP-dependent protein kinase I, *J. Biol. Chem. 265*, 4800−4808.
5. Anand, G. S., Hotchko, M., Law, D. S., Brown, S. H. J., Ten Eyck, L. F., Komives E. A., and Taylor, S. S. (2007) R-subunit isoform specificity in protein kinase A: distinct features of protein interfaces in PKA types I and II by amide H/2H exchange mass spectrometry, *Molecular Biology*, submitted for publication.
6. Herberg, F. W., Maleszka, A., Eide, T., Vossebein, L., and Tasken, K. (2000) Analysis of A-kinase anchoring protein (AKAP) interaction with protein kinase A (PKA) regulatory subunits: PKA isoform specificity in AKAP binding, *J. Mol. Biol. 298*, 329−339.
7. Vigil, D., Blumenthal, D. K., Taylor, S. S., and Trewhella, J. (2006) Solution scattering reveals large differences in the global structures of type II protein kinase A isoforms, *J. Mol. Biol. 357*, 880−889.
8. Viste, K., Kopperud, R. K., Christensen, A. E., and Doskeland, S. O. (2005) Substrate enhances the sensitivity of type I protein kinase A to cAMP, *J. Biol. Chem. 280*, 13279−13284.
9. Herberg, F. W., Dostmann, W. R., Zorn, M., Davis, S. J., and Taylor, S. S. (1994) Crosstalk between domains in the regulatory subunit of cAMP-dependent protein kinase: influence of amino terminus on cAMP binding and holoenzyme formation, *Biochemistry 33*, 7485−7494.
10. Hamuro, Y., Anand, G. S., Kim, J. S., Juliano, C., Stranz, D. D., Taylor, S. S., and Woods, V. L., Jr. (2004) Mapping intersubunit interactions of the regulatory subunit (RIalpha) in the type I holoenzyme of protein kinase A by amide hydrogen/deuterium exchange mass spectrometry (DXMS), *J. Mol. Biol. 340*, 1185−1196.
11. Kim, C., Xuong, N. H., and Taylor, S. S. (2005) Crystal structure of a complex between the catalytic and regulatory (RIalpha) subunits of PKA, *Science 307*, 690−696.
12. Anand, G. S., Hughes, C. A., Jones, J. M., Taylor, S. S., and Komives, E. A. (2002) Amide H/2H exchange reveals communication between the cAMP and catalytic subunit-binding sites in the R(I)alpha subunit of protein kinase A, *J. Mol. Biol. 323*, 377−386.
13. Bradford, M. (1976) A rapid and sensitive method for the quantitation of microgram quantities of protein utilizing the principle of protein-dye binding, *Anal. Biochem. 72*, 248−254.
14. Cook, P. F., Neville, M. E., Vrana, K. E., Hartl, F. T., and Roskoski, R. (1982) Adenosine cyclic 3′,5′-monophosphate dependent protein kinase: kinetic mechanism for the bovine skeletal muscle catalytic subunit, *Biochemistry 21*, 5794−5799.
15. Hibbs, R. E., Johnson, D. A., Shi, J., Hansen, S. B., and Taylor, P. (2005) Structural dynamics of the alpha-neurotoxin-acetylcholine-binding protein complex: hydrodynamic and fluorescence anisotropy decay analyses, *Biochemistry 44*, 16602−16611.
16. Birch, D. J. S., and Imhof, R. E. (1991) Time-Domain Fluorescence Spectroscopy Using Time-Correlated Single Photon Counting, in *Topics in Fluorescence Spectroscopy: Techniques* (Lakowicz, J. R., Ed.) Vol. 1, Plenum Press, New York.
17. Vigil, D., Blumenthal, D. K., Brown, S., Taylor, S. S., and Trewhella, J. (2004) Differential effects of substrate on type I and type II PKA holoenzyme dissociation, *Biochemistry 43*, 5629−5636.
18. Han, J., Liu, S., Rose, D. M., Schlaepfer, D. D., McDonald, H., and Ginsberg, M. H. (2001) Phosphorylation of the integrin alpha 4 cytoplasmic domain regulates paxillin binding. *J. Biol. Chem. 276*, 40903−40909.
19. Corbin, J. D., Brostrom, C. O., Alexander, R. L., and Krebs, E. G. (1972) Adenosine 3′,5′-monophosphate-dependent protein kinase from adipose tissue, *J. Biol. Chem. 247*, 3736−3743.
20. Rubin, C. S., Erlichman, J., and Rosen, O. M. (1972) Cyclic adenosine 3′,5′-monophosphate-dependent protein kinase of human erythrocyte membranes, *J. Biol. Chem. 247*, 36−44.
21. Beavo, J. A., Bechtel, P. J., and Krebs, E. G. (1974) Preparation of homogeneous cyclic AMP-dependent protein kinase(s) and its subunits from rabbit skeletal muscle, *Methods Enzymol. 38*, 299−308.
22. Reimann, E. M., Walsh, D. A., and Krebs, E. G. (1971) Purification and properties of rabbit skeletal muscle adenosine 3′,5′-monophosphate-dependent protein kinases, *J. Biol. Chem. 246*, 1986−1995.
23. Tao, M., Salas, M, L., and Lipmann, F. (1970) Mechanism of activation by adenosine 3′:5′-cyclic monophosphate of a protein phosphokinase from rabbit reticulocytes, *Proc. Natl. Acad. Sci. U.S.A. 67*, 408−414.
24. Kopperud, R., Christensen, A. E., Kjarland, E., Viste, K., Kleivdal, H., and Doskeland, S. O. (2002) Formation of inactive cAMP-saturated holoenzyme of cAMP-dependent protein kinase under physiological conditions, *J. Biol. Chem. 277*, 13443−13448.
25. Prinz, A., Diskar, M., Erlbruch, A., and Herberg, F. W. (2006) Novel, isotype-specific sensors for protein kinase A subunit interaction based on bioluminescence resonance energy transfer (BRET). *Cell. Signalling, 18*, 1616−1625.
26. Hofmann, F., Bechtel, P. J., and Krebs, E. G. (1977) Concentrations of cyclic AMP-dependent protein kinase subunits in various tissues, *J. Biol. Chem. 252*, 1441−1447.
27. Granot, J., Mildvan, A. S., Bramson, H. N., Thomas, N., and Kaiser, E. T. (1981) Nuclear magnetic resonance studies of the conformation and kinetics of the peptide-substrate at the active site of bovine heart protein kinase, *Biochemistry, 20*, 602−610.
28. Johnson, D. A., Leathers, V. L., Martinez, A. M., Walsh, D. A., and Fletcher, W. H. (1993) Fluorescence resonance energy transfer within a heterochromatic cAMP-dependent protein kinase holoenzyme under equilibrium conditions: new insights into the conformational changes that result in cAMP-dependent activation, *Biochemistry 32*, 6402−6410.
29. Yang, S., Fletcher, W. H., and Johnson, D. A. (1995) Regulation of cAMP-dependent protein kinase: enzyme activation without dissociation, *Biochemistry 34*, 6267−6271.

BI700421H